

Chemical sensing using nonoptical microelectromechanical systems

C. B. Freidhoff^{a)}

Electronic Sensor and Systems Sector, Northrop Grumman Corporation, Baltimore, Maryland 21203

R. M. Young, S. Sriram, T. T. Braggins, T. W. O'Keefe,^{b)} J. D. Adam, and H. C. Nathanson
Science and Technology Center, Northrop Grumman Corporation, Pittsburgh, Pennsylvania 15235

R. R. A. Syms, T. J. Tate, and M. M. Ahmad

Department of Electrical and Electronic Engineering, Imperial College, London SW7 2BT, United Kingdom

S. Taylor and J. Tunstall

*Department of Electrical Engineering and Electronics, Liverpool University,
Liverpool L69 3BX, United Kingdom*

(Received 27 October 1998; accepted 23 March 1999)

Micromachining is a technology that miniaturizes mechanical sensors and actuators through the use of tools and materials commonly used in the integrated circuit industry. The physics of the devices formed in this way are sometimes similar and sometimes different to achieve the same functionality of current macroscopic devices, but in sizes that are hundreds or thousands of times smaller. This article will discuss a few chemical detectors being developed as examples of the application of microelectromechanical systems (MEMS) for nonoptical laboratory instruments. In this article, we will report on the development and demonstration of two approaches (quadrupole and magnetic Lorentz) to fabricate a *mass filter* as part of a mass spectrometer. This article is not meant as a review of the field of MEMS chemical sensors, but rather a tutorial on how miniaturization is achievable through the use of MEMS fabrication techniques for mass spectrometers. © 1999 American Vacuum Society. [S0734-2101(99)15604-5]

I. INTRODUCTION

One of the dreams of microelectromechanical systems (MEMS) is to perform complex functions, such as those found in various life forms, on a silicon chip. This dream is possible due to the reduction in size of patterns that integrated circuit (IC) lithography tools can make ($<0.25 \mu\text{m}$), the complexity and speed of digital circuitry, and the understanding of material properties on the microscale level. Due to the use of IC lithography, miniaturization of devices is possible, such as the air bag sensor in modern automobiles. One of the abilities of living creatures that has gained a high emphasis in the microelectronics/MEMS arena is the sense of smell, i.e., the identification of molecules due to their interaction with other molecules and surfaces.

Current low-cost chemical sensors are generally specific in their detection capability, necessitating use of multiple devices in complex environments such as medical monitoring, internal combustion engines, the modern battlefield, or environmental air purity monitoring. The categorization of electronic forms of chemical sensors or noses is broken into five types: conductivity sensors, piezoelectric sensors, metal-oxide-semiconductor field effect transistors, optical sensors, and spectrometry-based sensing methods.¹ Examples of these are chem-resistors,¹ micromachined Fabry-Perot filters,² and single element surface acoustic wave detectors.¹ A good review on solid-state gas sensors has already been published³ and will not be covered in this article. Mass spectrometers/spectrographs are universal gaseous

chemical detectors, but have in the past been limited to laboratory use. Conventional mass spectrometers are bulky (bench-top or larger); they are heavy ($>50 \text{ kg}$), power hungry ($>1 \text{ kW}$), require highly trained technical personnel to operate, and interpret the results and expensive ($>\$10,000$). The critical components of mass spectrometers have been reduced down to micrometer (10^{-6}m) size dimensions through use of integrated micro-circuit lithography and micro-machining fabrication processes. Integration of these components will result in a universal chemical detection system with a 1000-fold reduction in size, weight, power, and cost.

In this article, we will report on the development and demonstration of two approaches to fabricate a *mass filter* as part of a mass spectrometer. This article is a tutorial on how miniaturization is achievable through the use of MEMS fabrication techniques for mass spectrometers.

II. BACKGROUND

The operations of a chemical sensing system can be divided into a number of blocks as shown in Fig. 1. This can apply to both biological, as well as instrumentation systems. For the human nose, the lungs act as the sample introduction pump, the epithelium sensory cells act as the chemical sensor, and the brain acts as the microprocessor and spectral library storage area.

A mass spectrometer is the chemical sensor under consideration in this article, but it is the combination of the mass spectrometer with a capable microprocessor and spectral library that allows an electronic version of the nose to be

^{a)}Electronic mail: carl_b_freidhoff@md.northgrum.com

^{b)}Posthumous.

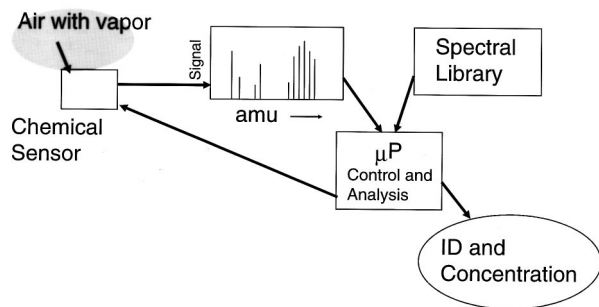


FIG. 1. Block diagram of chemical sensing systems.

implemented. A mass spectrometer determines the types of molecules present in a test gas by measuring the masses and quantities of the ionized products formed from energetic electron bombardment of the neutral vapor. Mass spectrometers do this by accelerating the ions through electric and/or magnetic fields to find the charge-to-mass ratio (e/m) of the ion. Resolutions of a fraction of an atomic mass unit (amu) over a range of one to several hundred amu, and capable of measuring several orders of magnitude in ion current or charge, can be found in common, bench-top laboratory instrument.

The sections of any mass spectrometer analysis system can be divided into seven components as shown in Fig. 2: (a) Dust filter, (b) sampling orifice, (c) ionizer, (d) ion optics, (e) mass filter, (f) ion detector and signal analyzer, and (g) vacuum pump.

Some of these have already been scaled down to micrometer (10^{-6} m) dimensions, notably the sampling orifice,⁴ (b), ionizer,^{5,6} (c), and ion optics,⁶ (d).

Among the laboratory mass spectrometers currently in use, the *quadrupole* is perhaps the most common in use today. A combination of direct current (dc) and radio frequency (rf) fields is generated on four rods, the alternating current (ac) component's frequency determining which e/m ratios are passed. By sweeping the fields, a range of masses can be scanned, with high resolution. Bench-top units use frequencies in the 2–18 MHz range, while scaling down to micrometer level parts will require boosting the frequency quite high, to the 2 GHz range to maintain adequate mass resolution for identification of samples.

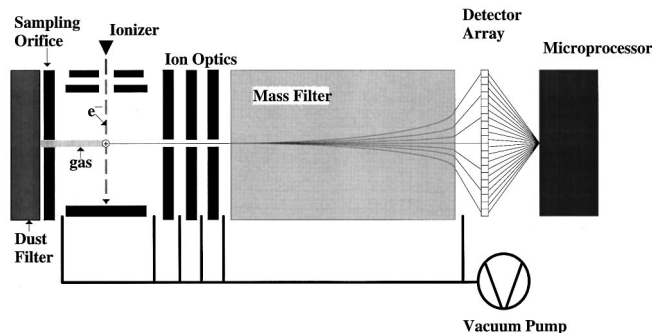


FIG. 2. Seven components of a mass spectrometer.

Mass spectrometers based on time of flight⁷ and ion mobility are also useful laboratory instruments. Charged species are produced by a pulsed ion source and arrive at a collection electrode over a period of time, and therefore determines their relative velocities. Scaling down to micrometer-level dimensions shortens the time domain available, implying an undesirably short time (femto-second) signal resolution requirement. Another mass spectrometer of the miniature scale whose theory has been presented in the literature is based on a traveling wave.⁸

However, an older e/m separation technique, one using magnetic (\mathbf{B}) fields, appears to scale well when reduced to micrometer sizes.⁹ Indeed, a great advantage over bench-top units can be gained in the micro-world. To create the required \mathbf{B} field of approximately 1 T (10 000 G), macro-world magnets end up being quite large in size and power usage. However, high fields near 1 T can easily be achieved using small gaps of a few hundred to few thousand micrometers between ordinary permanent magnets.

In a *magnetic sector* mass spectrometer, charged species are deflected into curved trajectories. These ions impinge on an array of spatially separate detectors, measuring the ion current collected. While the magnetic sector is simple in concept, its mass range is hardware limited and requires off-axis beam alignment. In a *Wien filter* configuration, crossed electrostatic and magnetic fields ($\mathbf{E} \times \mathbf{B}$) produce a constant velocity filtered ion beam.¹⁰ A Wien filter is a more compact mass spectrograph than the magnetic sector, and is scannable, as extra range and resolution can readily be obtained by sweeping the electric field. (Although resolution is not constant under the conditions of constant ion kinetic energy and fixed magnetic field.) Alternate means of scanning can include the ion kinetic energy and magnetic field.

This article will focus on the quadrupole and Wien filter approaches to separate ions and show progress made to date on the miniaturization of these devices through the use of micromachining fabrication techniques.

The small amount of sample being drawn through the orifice and the use of differential pumping techniques means that the requirements of the vacuum pump become minimal. An on-chip micromachine pump would be desirable for a truly portable unit. This is a system issue that will be covered in future publications, but will not be the focus of this article.

III. THEORY

Operation of a mass spectrometer, on either the macroscopic or microscopic regimes, requires that the ions that are formed follow well-defined trajectories. Collisions with walls or other gas molecules will result in deviations of the ion trajectory, cause beam broadening, and reduce the effective resolution and sensitivity of the device. A measure for the average distance that a molecule will travel between collisions is called the mean free path. For air at atmospheric pressure and room temperature, the mean free path of an ion is 65 nm and is inversely proportional to pressure. For successful operation of a mass spectrometer on a chip, a mean free path of an ion should be on the order of 1 cm (the length

of the spectrometers to be discussed), requiring the reduction of the pressure within the device to about 10 mTorr or 10^{-5} atm. This points out another advantage gained by micromachining, as this system pressure is some 1000 times larger than that tolerated in bench-top mass spectrometers, and eases the requirements of the vacuum pump.

Beam broadening can also be caused by space charge effects, which will limit the total signal that a particular geometry will be able to accommodate. Sample calculations of the space charge limit for an extremely narrow micromachined beam path with a $5\ \mu\text{m}$ beam diameter and 1 cm pole face length is 1 nA or 1 billion charges per second. This current is much, much greater than that required for a MEMS sensor on the millimeter scale, and hence, space charge limits to MEMS mass spectrometer sensitivity are generally not an issue.

IV. QUADRUPOLE MASS SPECTROMETER

The quadrupole mass spectrometer consists of an ionizer, a quadrupole electrostatic lens, and an ion counter. The device is operated under vacuum, and ions obtained by the ionization of residual gas are passed through the lens (which acts as a mass filter) to the detector. The lens consists of an assembly of four cylindrical electrodes, held accurately parallel with their centers on a square whose size is precisely related to their diameter. The application of voltages to diagonally opposed electrode pairs results in a close approximation to a hyperbolic potential field near the axis. The drive voltage contains both a dc and a rf component, whose amplitudes are scanned while being held in a fixed ratio. For a given voltage, only ions of a particular mass follow stable trajectories through the lens, so the output is a mass spectrum.

Conventional quadrupoles are bulky and fragile, have electrode diameters and lengths of approximately 5 mm and 10 cm, respectively, and require drive voltages sufficiently large that the lens is normally arranged as the capacitive part of an inductor-capacitor (L-C) resonator. Miniaturization has the potential to allow a reduction in the pumped volume, thus reducing cost, improving portability and extending the range of possible applications. However, miniaturization degrades sensitivity, since the ion flux is proportional to the area of the lens entrance pupil. Furthermore, higher drive frequencies are required, since the mass resolution depends on the number of rf cycles experienced by an ion traveling the length of the lens. It is also difficult to maintain the required constructional precision as the size of the assembly is reduced.

Despite these difficulties, a mass spectrometer based on a micro-engineered quadrupole has been constructed by collaboration between Imperial College and Liverpool University, UK.¹¹ The quadrupole is constructed from $500\ \mu\text{m}$ diameter Au metallized silica rods mounted in pairs on two Si dies, which are held apart by insulating rods as shown in Fig. 3. The correct electrode spacing is achieved through the use of V-shaped grooves as kinematic mounts. Each die carries one alignment rod, which mates with a groove on the other

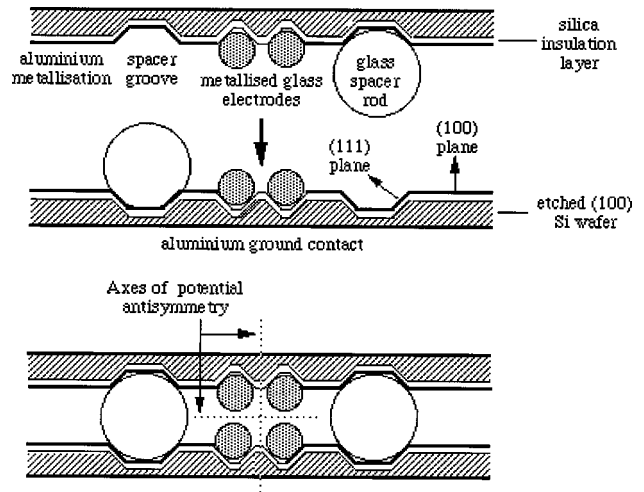


FIG. 3. Self-aligning microengineered quadrupole lens assembly.

die. Provided tangent plane contacts are made between the rods and the groove walls, this renders the electrode separation highly immune to variations in groove width. Because of the proximity of the grounded substrate to the axis, careful design is needed to obtain good electrostatic performance. A suitable design optimization procedure has been described earlier.¹²

A simple process for batch fabrication has been developed based on 3 in. diameter (100) oriented *p*-type Si wafers.¹³ V-shaped grooves are formed using an anisotropic etching in ethylene diamine pyrocatechol. After etching, the substrate is electrically isolated by a $1\text{-}\mu\text{m}$ -thick layer of thermal silica. Electrode contacts are defined by shadow-masked evaporation of Au. Windows are opened in the back side oxide, and a further Al layer is deposited as a ground contact. The electrodes are then bonded to the substrate with liquid indium metal. Each wafer contains sufficient dies to construct 8 lenses, with overall widths of 6 mm and lengths up to 3 cm. Tolerances in electrode position are 1%–3%, and are limited mainly by failure to seat the rods properly during bonding. Figure 4 shows the cross section of a pair of dies assembled to form a complete lens.

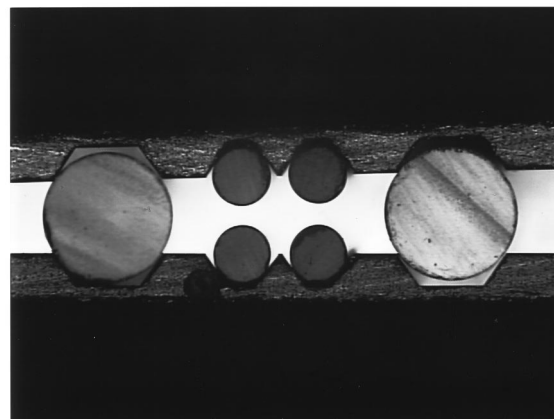


FIG. 4. Optical microscope view of cross section of an assembled lens.

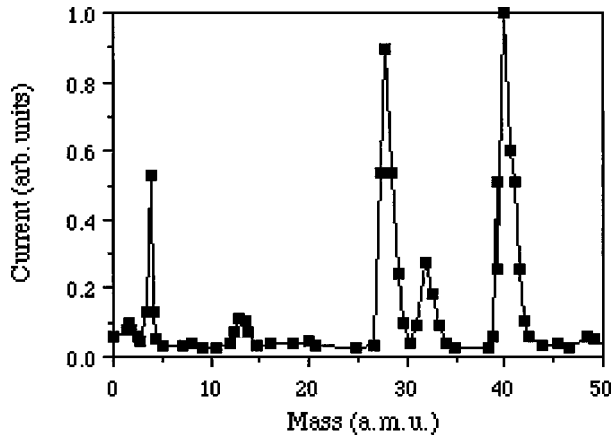


FIG. 5. Mass spectrum of a mixture of helium, argon, and air obtained with a 3 cm lens with 500 μm diameter electrodes, driven at 6 MHz.

Crude mass spectrometer action was first demonstrated using 2 cm long lenses coupled to a conventional VG Anavac ion source.^{14,15} More recently, enhanced resolution has been obtained using lenses with an optimized substrate topology and improved driver electronics.¹⁶ Figure 5 shows the mass spectrum of a mixture of argon, helium, and air obtained with a 3 cm lens driven at an rf frequency of 6 MHz. At mass 40, the resolution at 10% peak height is approximately 2.7 amu. Work is now in progress to develop a completely micro-engineered instrument with a self-aligned ion source, and to recover lost sensitivity using a quadrupole array.

Adequate resolution and throughput of a micro-quadrupole system can be achieved by scaling the rf frequency to match the dimensions of the quadrupole lens. In a paper by Austin, Holme, and Leck¹⁷ the mass range and the resolution limit of quadrupole mass spectrometers was given as functions of operating parameters. The resolution limit is given as

$$\Delta M = 4 \times 10^9 V_z / f^2 L^2, \quad (1)$$

where ΔM is the peak width in amu, V_z is the axial ion energy in electron volts, f is the applied frequency in Hertz, and L is the quadrupole length in meters. For a 3 cm quadrupole lens operating a 6 MHz, the resolution limit should be about 0.6 amu with a 5 eV beam energy. For a 1 cm quadrupole lens under the same conditions, the theoretical resolution limit would be 5.6 amu. This indicates that high resolution of 0.125 amu would require higher rf frequencies (16 MHz for a 3 cm long rod, 40 MHz for a 1 cm long rod, and 4 GHz for 0.1 mm long rod for 5 eV ion energies) to have resolutions with which standard laboratory quadrupoles typically operate. Assembly tolerances may also be playing a role in the lower than theoretical resolution achieved in experimental devices and possibly necessitate the use of lithography to align other components of the chemical sensor system with the quadrupolar lens.

The mass range of quadrupole mass filter systems follows the equation

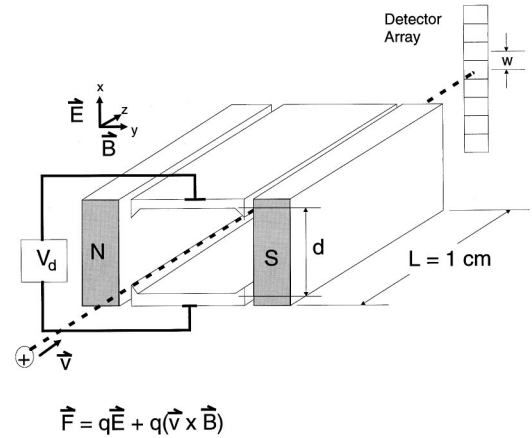


FIG. 6. Wien filter schematic, showing $\mathbf{E} \times \mathbf{B}$ fields and the detector spacing on the detector array (Δw).

$$M_m = 7 \times 10^6 V_m / f^2 r_0^2, \quad (2)$$

where r_0 is in meters (radius between rods) and V_m is the maximum value of the zero-to-peak rf voltage. For the 3 cm system, a mass range of approximately 300 amu would be achievable, assuming V_m is 400 VAC. Here is where a trade must be made. Higher resolution requires higher frequency. This will decrease mass range unless the limit on V_m is made higher through the use of thicker dielectrics. Changes in the rf voltage will follow the square of the frequency change.

V. WIEN FILTER MASS SPECTROMETER

Ions entering a perpendicular homogeneous magnetic field with the same kinetic energy will describe a circular path due to a force in the orthogonal direction ($\mathbf{F} = \mathbf{v} \times \mathbf{B}$). The radius of the arc of the path is dependent on the ion's mass-to-charge ratio. Imposing an electric field along this orthogonal permits further deflection of the ion beam (see Fig. 6) creating the so-called Wien Filter. This configuration has been previously used for isotope separation¹⁰ and is available commercially in a laboratory (Colutron 600B filter is 15.2 cm long and can generate up to 2500 G) size unit.¹⁸

Sample calculations of ion trajectories for dimensions of a miniaturized mass spectrometer are shown in Fig. 7. As can be seen, only a limited range of masses will be passed by the filter, and indeed too wide of a Wien Filter can result in extra loops in some lighter ion trajectories, producing spurious signals and degrading the desired mass ranges signal or sensitivity. Proper design can largely eliminate this problem. One of the features of the Wien configuration is that the magnetic field causes a focusing of the ions along a plane parallel to the end of the filter. This focusing is seen in the analysis shown in Fig. 7 for ions with different injection angles and is taken advantage of in the placement of the detector array and the operating parameters for the Wien filter.

The resolution of the Wien filter¹⁹ follows the equation

$$m / \Delta m = V_d L^2 / 2dV_i \Delta w, \quad (3)$$

where V_d is the deflection potential in volts, L is the length of the filter, d is the distance between the electrostatic field

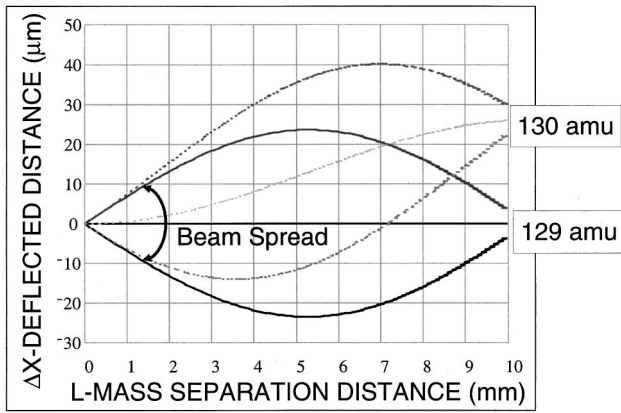


FIG. 7. Simulated ion trajectory plots done in two-dimensions show the focusing nature of the $\mathbf{E} \times \mathbf{B}$ field in the Wien filter that is used to optimize mass spectrometer design.

plates, V_i is the potential through which the ion is accelerated, and Δw is the spacing on the detector array. For a Wien filter that is 1 cm long with a 1 T magnetic field, ion energy of 5 eV, and a 22 μm spacing between detector elements, the theoretical resolution is 1 amu at approximately 580 amu. The high magnetic field is one of the features that scaling to small gaps allows a short mass filter to be achieved.

The assumption that is a part of this analysis of the Wien filter is that a homogeneous electrostatic and magnetic field exists in the device. This is easily done in laboratory where the aspect ratio of the cavity is close to one to one through the use of shim plates on the electrostatic field. The speed of the analysis is aided by taking advantage of the lateral width over which the ions are dispersed in a nearly linear fashion. This leads to a situation where the aspect ratio of the cavity of approximately 15–1 (1500 μm wide \times 100 μm high). If the cavity had the bare magnet poles that were electrically grounded, then a very nonuniform electrostatic field would exist. The insertion of the silicon chip containing the cavity allows one to control the electrostatic field by using the oxide of silicon to insulate between a number of “shim” plates that are fabricated on top of the silicon dioxide and connected on-chip using thin film resistors. The ultimate limit of

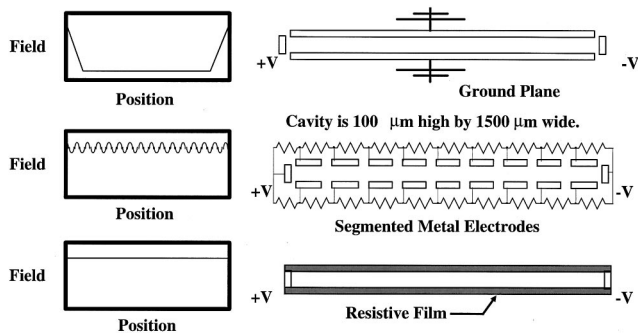


FIG. 8. Effect on the uniformity of the electrostatic field is qualitatively illustrated here starting with electrostatic field plates between two electrically grounded magnet poles to the segmented field plates and the resistive film electrode design.

TABLE I. Electrostatic field for a mass filter needs to have a uniformity of 0.25% or better to obtain mass resolutions of 1 amu at 200 amu with a Wien filter.

Ion mass for unit amu resolution	Electric field uniformity (%)
20	2.4
50	1
100	0.5
200	0.25

this would be the use of an appropriate resistive film that would act as an “infinite” number of shims. These are illustrated in Fig. 8.

In order to resolve two adjacent masses, the electrostatic field, \mathbf{E} , can not have variations greater than the difference in \mathbf{E} required to balance the electrostatic and magnetic forces for each mass. At balance, let

$$v_m * B = E_m \quad \text{and} \quad (4)$$

$$v_{m+1} * B = E_{m+1}, \quad (5)$$

where v_m is the velocity of ion with mass m , E_m is the electrostatic field to balance the magnetic field B , so that the ion with mass m can traverse the mass filter without being deflected. The fractional difference between E_m and E_{m+1} is

$$\frac{E_m - E_{m+1}}{E_m} = \frac{v_m * B - v_{m+1} * B}{v_m * B} = 1 - \frac{v_{m+1}}{v_m}. \quad (6)$$

The kinetic energy of the ions is assumed to be the same, so

$$v_m = \sqrt{\frac{2 * q * V_a}{m}}, \quad (7)$$

where q is the charge on the ion. Substituting Eq. (6) into Eq. (7) gives

$$\frac{\Delta E_{m,m+1}}{E_m} = 1 - \frac{\sqrt{\frac{2 * q * V_a}{m+1}}}{\sqrt{\frac{2 * q * V_a}{m}}} = 1 - \sqrt{\frac{m}{m+1}}. \quad (8)$$

The uniformity of the electrostatic field can then be determined for a number of resolving powers. Some of the values for uniformity are given in Table I.

Modeling of the electrostatic field was performed by a number of electrostatic modelling programs and the results are plotted in Fig. 9. The maximum dimension of the shims must be less than the cavity height. In Fig. 9, the point indicated as seven shims exceeds the maximum dimension and is not included in the data fits to determine the required number of shims. Both a linear and logarithmic fit were applied to the data. Here, one can see that the number of shims required would require be between 48 (linear result) and 64 (logarithmic result). For a 1500 μm wide cavity and equal spacing of the metal lines and gaps, the widths of the lines and spaces would be approximately 11.5–15 μm . This does not seem small for IC standards, but the lines must be maintained over

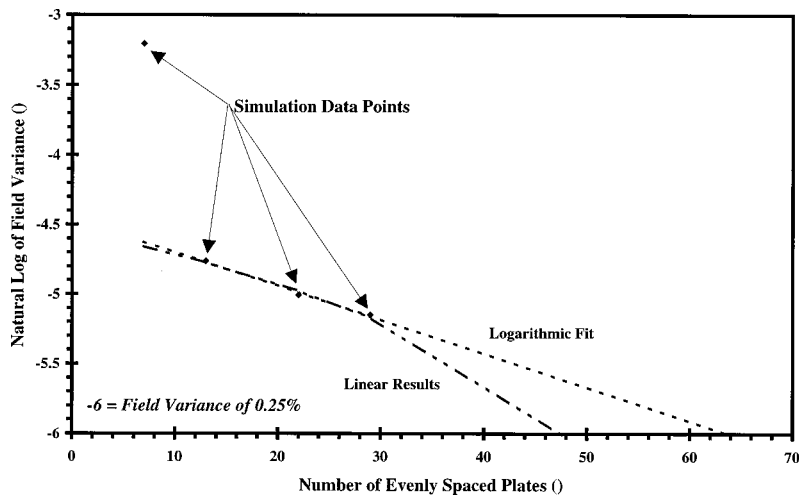


FIG. 9. Estimate of the number of evenly spaced metal grid plates for both the linear fit results and logarithmic fit results is plotted.

a length of 1 cm, which is difficult to do cost effectively in IC fabrication. This forced the consideration of resistive films, and undoped polysilicon was tested and found to be excellent for this application. No charging of the surface has been noted in any of our tests. The mass spectra taken with a 1 cm long Wien filter are shown to improve as the electrostatic field was made more uniform as illustrated in Figs. 10(a) and 10(b). Further improvements would be achieved by shaping the electrostatic fields at the entrance and exit points of the Wien filter to match the diverging magnetic fields at these areas. This is being planned in future mask sets. At this time, the practical resolution for a Wien filter

that is 1 cm long with a 1 T magnet is estimated to be between 350 and 400 amu due to the grain size of the polysilicon film causing deviations from the ideal electrostatic field.

Implementation of the electrode scheme in the silicon Wien filter is shown in Figs. 11(a) and 11(b). Figure 11(a) shows a photograph of a silicon micromachined mass filter half with seven segmented electrostatic field. Figure 11(b) is an photograph of silicon micromachined mass filter half with a resistive film with a depth of 40 μm , width of 1500 μm , and length of 10 000 μm .

The mass filter components (all mass filter components were 1 cm long) with both segmented metal plates and a resistive film were tested in a laboratory vacuum chamber using a hot cathode ion source adapted from a Varian MS 9 leak detector and a continuous dynode electron multiplier (DeTech Model 206.5EIC) as the detector. Xenon gas was used due to its isotope pattern to determine mass resolutions achieved. The results are shown in Figs. 10(a) and 10(b) for the seven segment and resistive film mass filters, respectively. A calibrated electromagnet was used to allow unfiltered beams to be used to align the ion beam without a magnetic field present. The magnetic field generated for these mass spectra was approximately 0.8 T. As can be seen the improvement in resolution is clearly noticeable, the electrostatic field plate with the seven segment electrodes obtains a resolution of about 80 amu, whereas the resistive film test exhibited a resolution of approximately 150 amu. Improvements in resolution are expected when smaller entrance slits and the detector array is used.

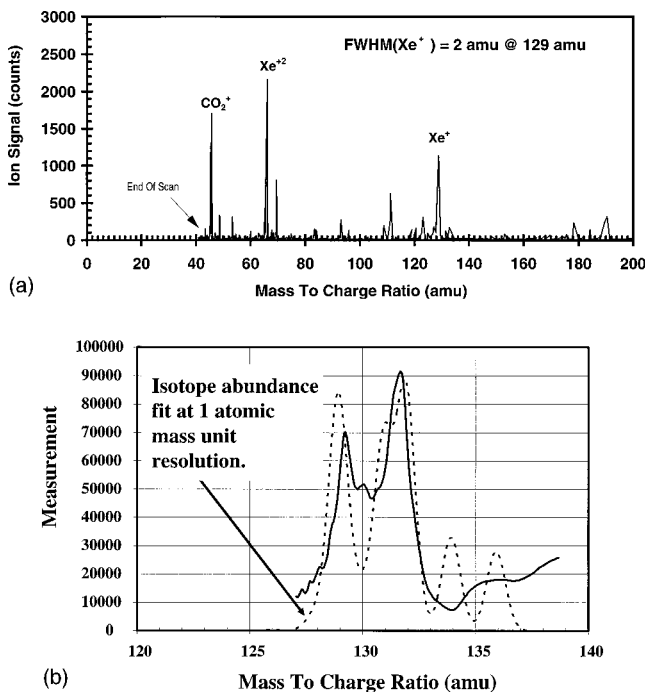
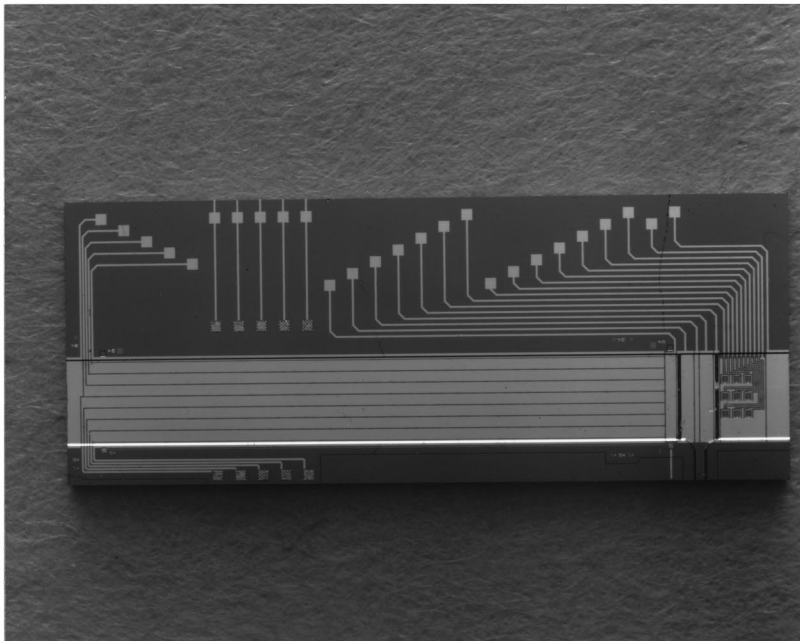


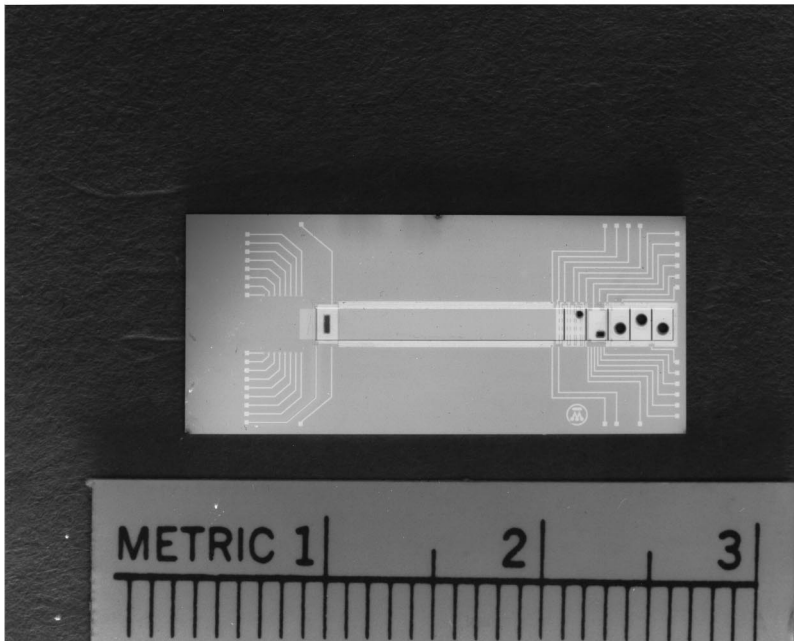
FIG. 10. (a) Mass spectrum taken with a silicon Wien filter with the electrostatic field plates divided into seven metal segments. The resolution achieved was roughly 1 amu at 80 amu. (b) The mass spectrum of xenon taken with a silicon Wien filter is plotted along with a simulated spectrum of the natural isotope pattern with a resolution of 1 amu at 150 amu.

VI. SUMMARY

Strides have been made in the miniaturization of mass filters. Other components of a mass spectrometer have also been miniaturized and demonstrated, notably the ionizer and detector. Integration of these components with the mass filter is the next step in the production of portable chemical detectors. Miniaturization has not meant the loss of performance in order to achieve a portable unit at least in terms of the



(a)



(b)

FIG. 11. (a) Silicon Wien filter with the seven segment filed plates (1 cm long) shows the integration that can be achieved using micromachining techniques. The ions travel from the ionizer region on the right of each picture. A simple three element Einzel lens was part of this design. (b) A microphotograph of a half of the mass spectrograph chip with the resistive film electrostatic field plate and the vacuum manifold holes. The resistive film simplifies the lithography requirements in the mass filter region and provides a nearly ideal electrostatic field. A double zoom lens (nine elements) was added in place of the Einzel lens in this design.

mass filters as presented in this article. MEMS fabrication allows the vast reduction in the size of parts required for the chemical sensor and with batch fabrication will allow low cost units to be produced if reasonable volumes are achievable.

ACKNOWLEDGMENTS

This work on the Wien filter approach has been supported by the Northrop Grumman Corporation and the Defense Advanced Projects Research Administration/Department of Energy through cooperative agreement No. DE-FC08-94ID13292. The authors would like to thank Dr. K. Gabriel,

Dr. M. Donlon, Dr. E. Bragg, and K. Price for their useful comments and support. The work at Northrop Grumman would not have been possible without the Central Processing Laboratory staff. In particular, the following technical staff personnel contributed significantly to the development of the MEMS Wien filter and so the authors thank Rich Sabol, Carl Seiler, Joseph Kotvas, and Mike Testa for their personal involvement in this work.

¹H. T. Nagle, R. Gutierrez-Osuna, and S. S. Schiffman, *IEEE Spectr.* **35**, 22 (1998).

²H. Alause, F. Grasdepot, J. P. Malzac, W. Knap, and J. Hermann, *Sens. Actuators B* **43**, 18 (1997).

- ³A. M. Azad, S. A. Akbar, S. G. Mhaisalkar, L. D. Birkefeld, and K. S. Goto, *J. Electrochem. Soc.* **139**, 3690 (1992).
- ⁴R. W. Tjerkstra, M. de Boer, E. Berenschot, J. G. E. Gardeniers, A. van den Berg, and M. Elwenspoek, *Proceedings of the IEEE International Workshop on MEMS*, IEEE 97CH36021, Nagoya, Japan, 1997, pp. 147–152.
- ⁵G. G. P. van Gorkom and A. M. E. Hoeberechts, *Inst. Phys. Conf. Ser.* **99**, 41 (1989).
- ⁶T. H. P. Chang *et al.*, *J. Vac. Sci. Technol. B* **8**, 1698 (1990).
- ⁷W. A. Bryden, R. C. Benson, S. A. Ecelberger, T. E. Phillips, R. J. Cotter, and C. Fenselau, *Johns Hopkins APL Tech. Dig.* **16**, 296 (1995).
- ⁸A. Feustel, J. Müller, and V. Relling, *A Microsystem Mass Spectrometer*, *Micro Total Analysis Systems*, edited by A. van der Berg and P. Bergvelt (Kluwer Academic Publishers, Amsterdam, 1995), pp. 299–304.
- ⁹C. B. Freidhoff, R. M. Young, and S. Sriram, U.S. Patent No. 5,386,115 (Jan. 31, 1995).
- ¹⁰L. Wahlin, *Nucl. Instrum. Methods* **27**, 55 (1967).
- ¹¹S. Taylor, R. R. A. Syms, H. A. Dorey, and T. J. Tate, British Patent No. 9506972.0 (1995).
- ¹²R. R. A. Syms, T. J. Tate, M. M. Ahmad, and S. Taylor, *IEEE Trans. Electron Devices* **TED-45**, 2304 (1998).
- ¹³R. R. A. Syms, T. J. Tate, M. M. Ahmad, and S. Taylor, *Electron. Lett.* **32**, 2094 (1996).
- ¹⁴S. Taylor, J. J. Tunstall, R. R. A. Syms, T. J. Tate, and M. M. Ahmad, *Electron. Lett.* **34**, 546 (1998).
- ¹⁵S. Taylor, J. J. Tunstall, T. J. Tate, R. R. A. Syms, and M. M. Ahmad, *Proceedings of the 1998 IEEE International Workshop on MicroElectro-Mechanical Systems*, Heidelberg, Germany, 25–29 January 1998, pp. 438–442.
- ¹⁶S. Taylor *et al.*, *Proceedings of the 14th International Vacuum Congress*, Birmingham, 31 Aug.–4 Sept. 1998.
- ¹⁷W. E. Austin, A. E. Holme, and J. H. Leck, in *Quadrupole Mass Spectrometry and its Applications*, edited by P. H. Dawson (Elsevier, Amsterdam, 1976), Chap. VI.
- ¹⁸Colutron Corporation, Boulder, Colorado 80301.
- ¹⁹J. H. Moore, C. C. Davis, and M. A. Coplan, *Building Scientific Apparatus*, 2nd ed. (Addison-Wesley, New York, 1989).